International Journal of Energy and Power Engineering
2021; 10(5): 87-95
http://www.sciencepublishinggroup.com/j/ijepe
doi: 10.11648/j.ijepe.20211005.12
ISSN: 2326-957X (Print); ISSN: 2326-960X (Online)

Numerical Analysis of $CsSnGeI_3$ Perovskite Solar Cells Using SCAPS-1D

Titu Thomas

Department of Physics, Nirmala College, Muvattupuzha, India

Email address:
titu1thomas@gmail.com

To cite this article:
Titu Thomas. Numerical Analysis of $CsSnGeI_3$ Perovskite Solar Cells Using SCAPS-1D. *International Journal of Energy and Power Engineeringh.* Vol. 10, No. 5, 2021, pp. 87-95. doi: 10.11648/j.ijepe.20211005.12

Received: September 22, 2021; **Accepted**: October 19, 2021; **Published**: October 29, 2021

Abstract: Recently, organic-inorganic perovskite-based solar cells have become promising devices due to their unique properties in the photovoltaic field. However, the factor of toxicity, stability, high production cost and complicated fabrication processes of these devices is a challenge to their progress in commercial production. Here a numerical modelling of Caesium Tin–Germanium Tri-Iodide ($CsSnGeI_3$) as an efficient perovskite light absorber material is carried out. In this paper, different inorganic Hole Transport Materials (HTMs) such as Cu_2O, CuI, $CuSbS_2$, CuSCN and NiO have been analyzed with C_{60} as the Electron Transport Material (ETM). We intend to replace the conventional hole and electron transport materials such as TiO_2 and Spiro-OMeTAD which have been known to be susceptible to light induced degradation. Moreover, the influence of the Electron Transport Layer (ETL) and the perovskite layer properties, bandgap, doping concentration and working temperature for various Hole Transport Layers (HTL) on the overall cell performance have been rigorously investigated. The design of the proposed PSC is performed utilizing SCAPS- 1D simulator and for optimum device an efficiency greater than 30% was obtained. The results indicate that $CsSnGeI_3$ and C_{60} are viable candidates for use as an absorber layer and electron transport layer in high-efficiency perovskite solar cells, with none of the drawbacks that other PSCs have.

Keywords: Perovskites, SCAPS, $CsSnGeI_3$

1. Introduction

Photovoltaic (PV) devices which convert solar energy into electrical energy are the alternatives to reduce carbon emissions while meeting the increased demand in energy consumption. With a power conversion efficiency (PCEs) exceeding 26% [1] and long- term durability, High-purity crystalline silicon is an ideal product for the market. However, as a result of the rigorous research in this field various other PV technologies, especially on thin films (<1 mm) based on simple deposition methods have emerged. This promises a reduction in production cost and production of high-quality semiconductors. Recently, perovskite solar cells (PSCs) have emerged as one such candidate [2-4]. In just a few years, the efficiency of perovskite solar cells has crossed the 22% mark of CdTe solar cells. [5]

Perovskite, named after the Russian scientist L.A. Perovski [6], has a crystal structure ABX_3 (X = oxygen, halogen). With the larger cation A occupying a cubo-octahedral site shared with twelve X anions and the smaller B cation in an octahedral site sharing six X anions [7]. Basically perovskite solar cells are solid-state sensitized solar cells based on dye-sensitized Gratzel solar cells [8]. Although the perovskites exhibit unique optoelectronic properties like high absorption coefficient [9] in the UV visible spectrum, tuneable bandgap, large charge carrier mobility, long charge carrier diffusion length [10], defect tolerance property and so on they have some major drawbacks. One of the major disadvantage is their thermal instability caused by the photobleaching effect, moisture and oxygen induced degradation etc. this reduces their compound shelf life. Also other problems like instability due to the presence of organic cations, anomalous hysteresis, presence of toxic chemicals like lead and problems with large area flexible PV systems are also yet to be pondered [11].

Not only have the organic-inorganic hybrid absorber materials, organic charge transport materials such as Spiro-OMeTAD [12], P3HT [13] become unstable in the presence of oxygen, light, and moisture [14]. Besides that, several organic charge transport materials react with perovskite material, show hostile behavior due to hygroscopic materials,

low mobility [15] and have high preparation costs. For these disadvantages, researchers are looking forward to inorganic charge transport materials as they provide good transparency in ultraviolet, visible and infrared spectrum, wide bandgap, high charge carrier mobility [16], superior thermal [17] and chemical stability, and simple synthesizing process [16].

Scientists have been trying to work in this hostile behavior of perovskite solar cells on various aspects and to develop superior perovskite materials with superior thermal [18] and chemical stability, simple synthesizing process [19] and most importantly less toxic. Two approaches are usually followed in this regard. Firstly, mixing lead with other metals which have lower toxicity such as tin-lead alloyed perovskite ($CH_3NH_3SnxPb1$-x) [20] and secondly by completely replacing lead with analogous metals [20]. Several low-toxicity cations have been proposed for replacing Pb(II) in halide perovskites [21], including Ag(I) [22], Bi(III) [23], Sb(III) [24], Ti(IV) [25], Ge(II) [26], and Sn(II) [27]. Among these candidates, Tin is considered more suitable material because both are in the same group in periodic table and halide perovskites based on Sn(II) have shown the highest PCE, and, thus, have attracted the most attention in the PSC field. Typical Sn-based halide perovskites that have been studied include $CH_3NH_3SnI_3$ ($MASnI_3$), $HC(NH_2)_2SnI_3$ ($FASnI_3$) [28], and $CsSnI_3$ [29]. Among other candidates Min Chen et al [30] proposed a nontoxic perovskite absorber material $CsGeSnI_3$. While PSCs based on $MASnI_3$ and $FASnI_3$ perovskites have been shown to deliver high PCE, up to 9% [31], these materials have intrinsically low stability [32]. This is primarily attributed to the presence of the organic cation, which is prone to facile volatilization.

In this work, for the first time we investigate the simulation of $CsSnGeI_3$ based perovskite solar cells [33, 34] with different materials as their Electron Transport Layer (ETL) and Hole Transport Layer (HTL) layers using the SCAPS 1-D simulation software. We study the impact of the change in various parameters of the HTL and absorber layers in the overall performance of the device. Also, the effect on properties of the solar cell with the change in operating temperature is studied as well.

2. Simulation Method

2.1. Device Simulation Methodology

Numerical simulation has a great importance in understanding the physical properties and design of solar cells. It can interpret the measurements on complex structures, design and optimisation of advanced cell structures. There are various simulation packages like SILVACO ATLAS, AMPS, COMSOL etc in the market [35]. Here we use the Solar Cell Capacitance Simulator (SCAPS) software version 3.2.00 for the simulation. It is developed by Prof. Marc Burgelman [36] at the Department of Electronics and Information Systems (ELIS) of the University of Gent, Belgium. In SCAPS various material parameters like thickness, band gap, permittivity, mobility etc and operating conditions like temperature, voltage, frequency, illumination can be set [37]. The uniqueness of SCAPS is that it can calculate almost all the parameters like spectral response, energy bands, ac characteristics, J-V curve and defect density [38-40] by just solving three basic semiconductor equations: continuity equations for both electron and holes and Poisson equation [41]. The basic sequence of operation of SCAPS software [42] is illustrated in Figure 1.

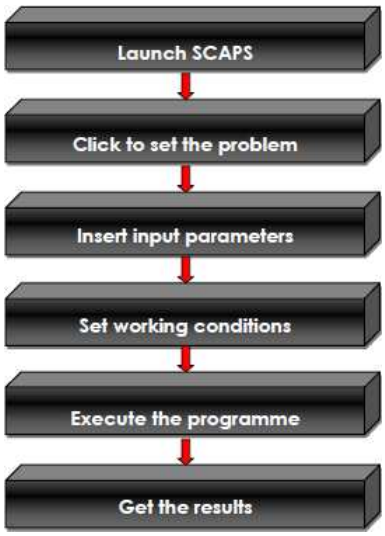

Figure 1. *Basic sequence of the SCAPS Simulation process.*

2.2. Device Architecture

The simulated PSC has five layers: (i) Gold (Au) as the metal contact (ii) The p-type Hole Transport Layer (HTL) CuSCN, $CuSbS_2$, NiO, Cu_2O and CuI (iii) Absorber layer as $CsGeSnI_3$, (iv) The Electron Transport Layer (ETL) as C_{60} (v) Transparent Conducting Oxide. So basically here we simulate five device configurations $Au/CuSCN/CsGeSnI_3/C_{60}/TCO$, $Au/CuSbS_2/CsGeSnI_3/C_{60}/TCO$, $Au/CuI/CsGeSnI_3/C_{60}/TCO$, $Au/Cu_2O/CsGeSnI_3/C60/TCO$ and $Au/NiO/CsGeSnI_3/C_{60}/TCO$. The schematic of the device and the energy level diagram of the proposed structures is shown in Figures 2 and 3 respectively. The absorber material should have high hole and electron mobility since it needs to absorb incident radiation leading to the creation of charge carriers, while the ETL and HTL layers extract and transfer electrons and holes respectively.

2.3. Device Simulation Parameters

The parameters for different layers in the simulation are chosen on the basis of theoretical considerations, experimental data and existing literature or in some cases, reasonable estimation [43-48], [37], Table 1 summarizes the simulation parameters for the configuration. In the given parameters Eg is the energy bandgap, ϵr is the relative permittivity, χ being the electron affinity, μn and μp are the electron and hole nobilities respectively. N_A and N_D are the densities of acceptor and donor materials whereas N_C and N_V are the effective densities of conduction band and valence

band. The parameter values not included in the table are set identical for all layers. Neutral Gaussian distribution defect is adopted with characteristic energy being set to 0.1 eV [48]. The electron and hole capture cross section is set to 9×10^{-15} cm^2 with the thermal velocity of both carriers fixed at 10^7 cm/s [49-51].

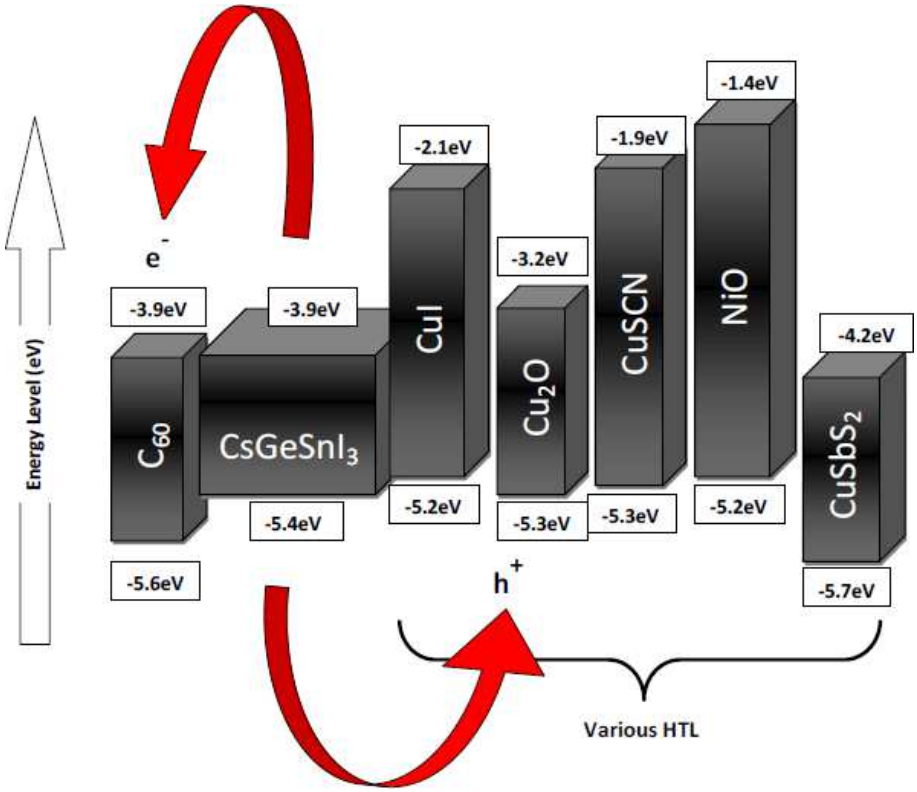

Figure 2. *Energy band diagram of the proposed device.*

Table 1. *Parameters of window layer, buffer layer and absorber layers for simulation.*

Parameters	C_{60}	$CsGeSnI_3$	CuSCN	$CuSbS_2$	Cu_2O	CuI	NiO
Eg (eV)	1.7	1.5	3.4	1.58	2.17	2.98	3.8
χ (eV)	3.9	3.9	1.9	4.2	3.20	2.1	1.46
N_c (cm^{-3})	8×10^{9}	2.2×10^{18}	2.2×10^{18}	2×10^{18}	2×10^{17}	1×10^{22}	2.8×10^{19}
N_v (cm^{-3})	8×10^{9}	1.8×10^{19}	2.9×10^{19}	1×10^{19}	1.1×10^{19}	1×10^{22}	10^{19}
N_D (cm^{-3})	2.6×10^{18}	--	-	--	--		--
N_A (cm^{-3})	-	1×10^{14}	10^{18}	1.38×10^{18}	1×10^{18}	2×10^{18}	10^{18}
ε_r	4.2	9	9	8.2	7.11	6.5	10.7

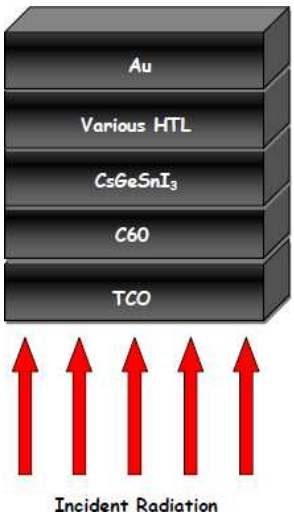

Figure 3. *Device structure.*

3. Results and Observations

3.1. Effect of the Bandgap of the Absorber Layer

The effect of band gap on the various solar cell characteristics has been examined since the band gap of a perovskite absorber is a significant parameter [52, 53]. In this study the band gap is adjusted from 1.2eV to 2.0eV. When the band gap is 1.2eV, the V_{oc} and J_{sc} have maximum values of 1.38V and 36mA/cm^2 respectively, as shown in Figure 4, and then both drop. Because the absorption of photons with energy greater than the band gap (which contributes to the photocurrent) diminishes as the band gap increases, the Jsc continues to drop. PCE follows the same trend as J_{SC}, and it drops to just 8% at higher band gaps (as illustrated in Figure 3(c)). The FF remains a constant for lower values of band gap but ultimately falls off at higher values. From the observations we conclude that, as the band gap of perovskite

increases the light harvesting property of the solar cell goes on worsening.

3.2. Effect of the Acceptor Density of the Absorber Layer

As the doping of the absorber layer increases, more carriers can contribute to reverse saturation current causing its rise. According to the diode circuit model, the V_{OC} can be expressed as [54]

$$V_\alpha = \frac{nkT}{q}\, log\left(\frac{Jsc}{J_0} + 1\right)$$

Here, n is representing the ideality factor, k denotes the Boltzmann constant, T is used to denote the temperature, J_0 and q is the reverse saturation current and charge respectively. It can illustrate that due to increase in temperature, the value of J_0 rises exponentially which leads to the reduction in open circuit voltage. From another point of view, when doping concentration increases, the electric field at the perovskite interface increases and the separation process will be enhanced. However, increasing recombination according to this increasing field will badly affect the performance. In this scenario most of the devices show similar decrement type of behaviour on various parameters except $CuSbS_2$. As indicated in Figure 5, the open circuit voltage (V_{oc}), FillFactor and power efficiency reach a maximum value of 1.33V, 90.2% and 30.1% respectively at doping concentration of 10^{16} cm $^{-3}$, and then decrease. While the J_{sc} almost remains a constant at 25mA/cm^2. The optimum value of doping concentration (N_A) was set to 10^{15} cm^{-3}.

3.3. Effect of the Donor Density of the ETL Layer

Donor density or charge carrier density of ETL layers of each solar cell had been varied between 10^{16} cm^{-3} and 10^{20} cm^{-3} as shown in Figure 6 to find variation in Efficiency, V_{oc}, J_{sc} and FF of the solar cells. For all of the solar cells, when we vary the acceptor density between 10^{15} cm^{-3} and 10^{20} cm^{-3} can see that J_{sc} decreased but V_{oc}, FF, and Efficiency increased with the increase of acceptor density. For increasing donor density of the absorber layer, J_{sc} decreased from 25.5mA/cm^2. From the PN-junction model, we can find the equation [55]

$$J_0 = Aqn_i^2\left(\frac{D_n}{L_n N_a} + \frac{D_p}{L_p N_d}\right)$$

Where, A is the quality factor of the diode, J_0 is the reverse saturation current density, n_i is the intrinsic concentration, q is the electronic charge, L is the diffusion length, D is the diffusion coefficient, N_a and N_d are the donor and acceptor doping concentrations respectively and the subscripts p and n refer to holes and electrons respectively. When N_d increases, the saturation current J_0 will decrease according to the above equation. And when J_0 decreases, V_{oc} increases. Increased carrier concentration, on the other hand, promotes the recombination process by introducing recombination centres or traps into the layer, which reduces the ability of photogenerated carriers to be collected at the front, lowering Jsc. Again, as V_{oc} increases, PCE and FF also increase for all of the solar cells Cu_2O, CuI and NiO based solar cells all had almost the same maximum PCEs of 33%.

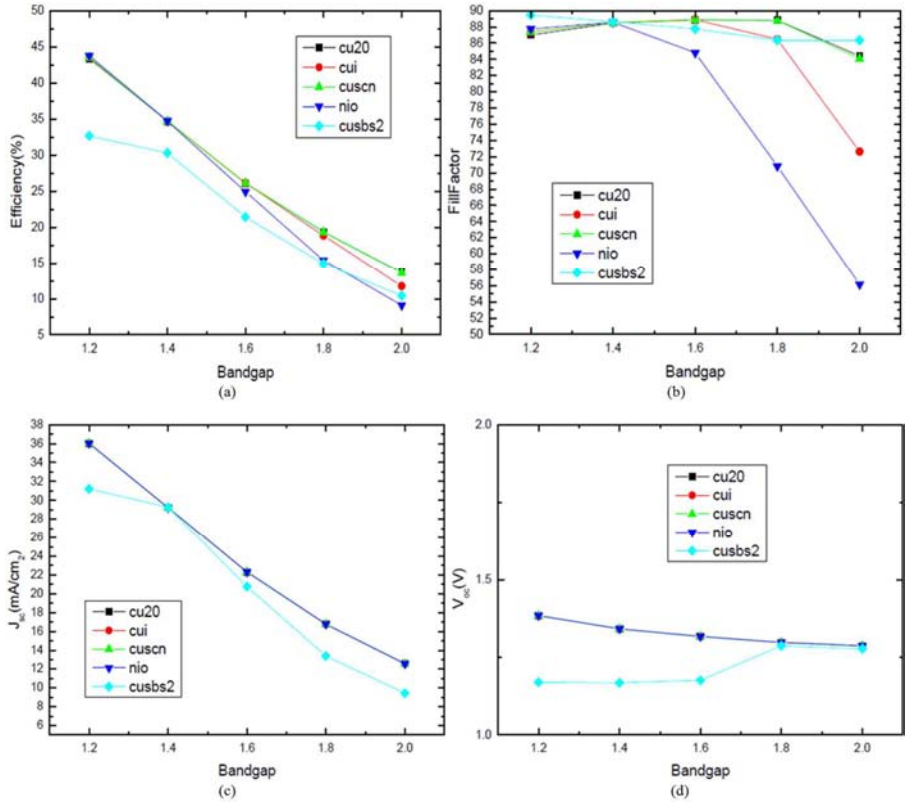

Figure 4. *Effect of changing bandgap of buffer layer on solar cell basic parameters (a) PCE (b) FillFactor (c) J_{sc} and (d) Voc.*

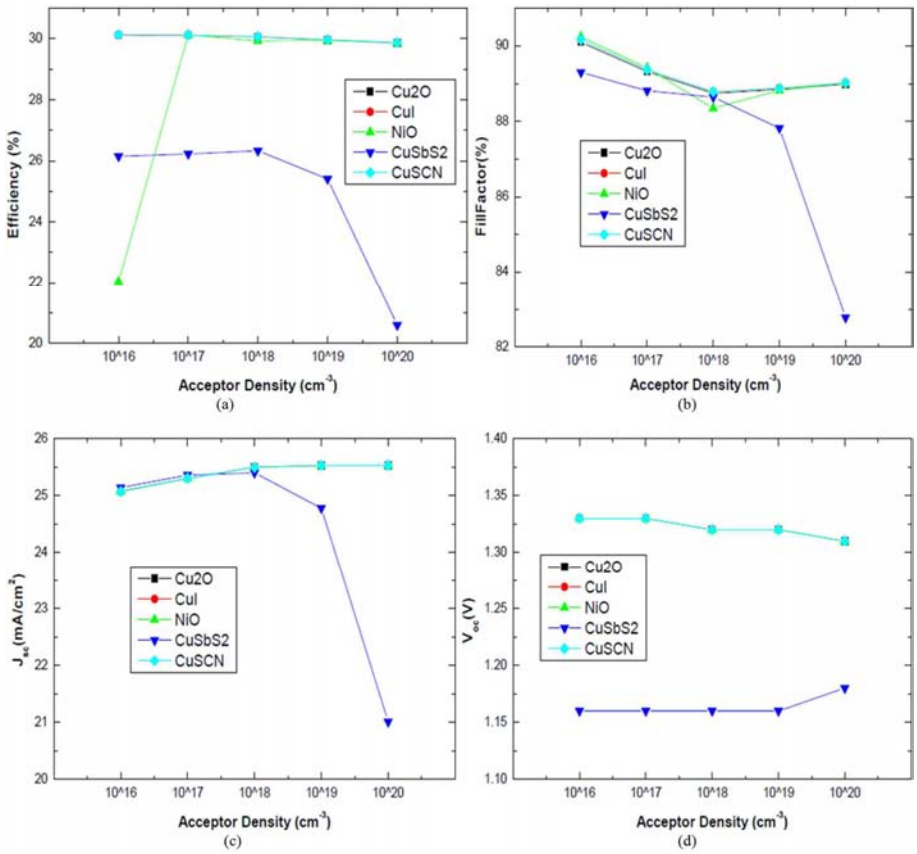

Figure 5. *Device properties (a) PCE (b) Fill Factor (c) J_{sc} and (d) Voc as a function of increasing Acceptor Densities of the perovskite layer.*

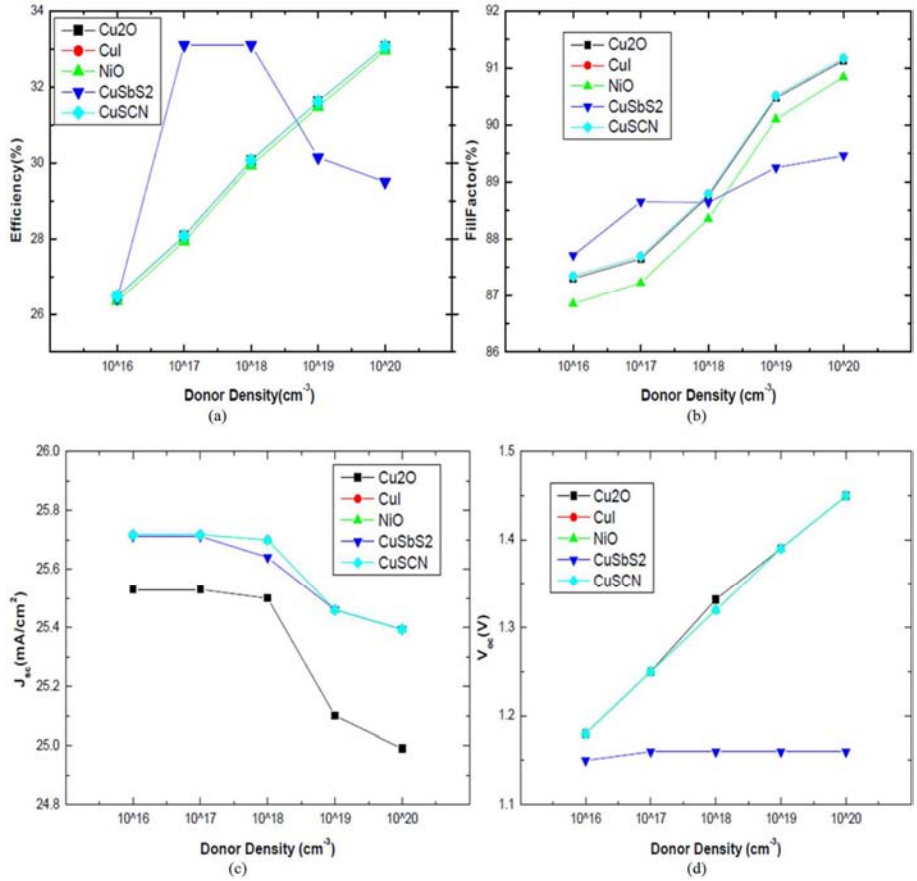

Figure 6. *Device properties (a) PCE (b) FillFactor (c) J_{sc} and (d) Voc as a function of increasing Donor Densities of the perovskite layer.*

3.4. Effect of Temperature on the Device

Here we studied the change in the temperature of a solar cell and its impact on the overall performance of the cell. At first we kept the temperature at 300 K in the simulation. Then the temperature was changed from 300 to 400 degrees Celsius to take into account the influence of the working temperature on the PCE, Voc, Jsc and FF of all solar cells, for the ideal absorbent layer and the thickness of the buffer layer. Figure 7 shows that the current density remains relatively constant with increasing temperatures, although the Voc, PCE and FillFactor of the PSC decrease. This might be due to the thermal dissociation of the absorbent layer [58]. Generally, increased temperature affects parameters such as carrier mobility, electron and hole concentration and band gap of the materials that changes the resistance and thus, PCE, V_{oc} and FF get declined. When the temperature was increased to 400 K, the efficiency of the device decreased to 24.87% for most of the devices except $CuSbS_2$.

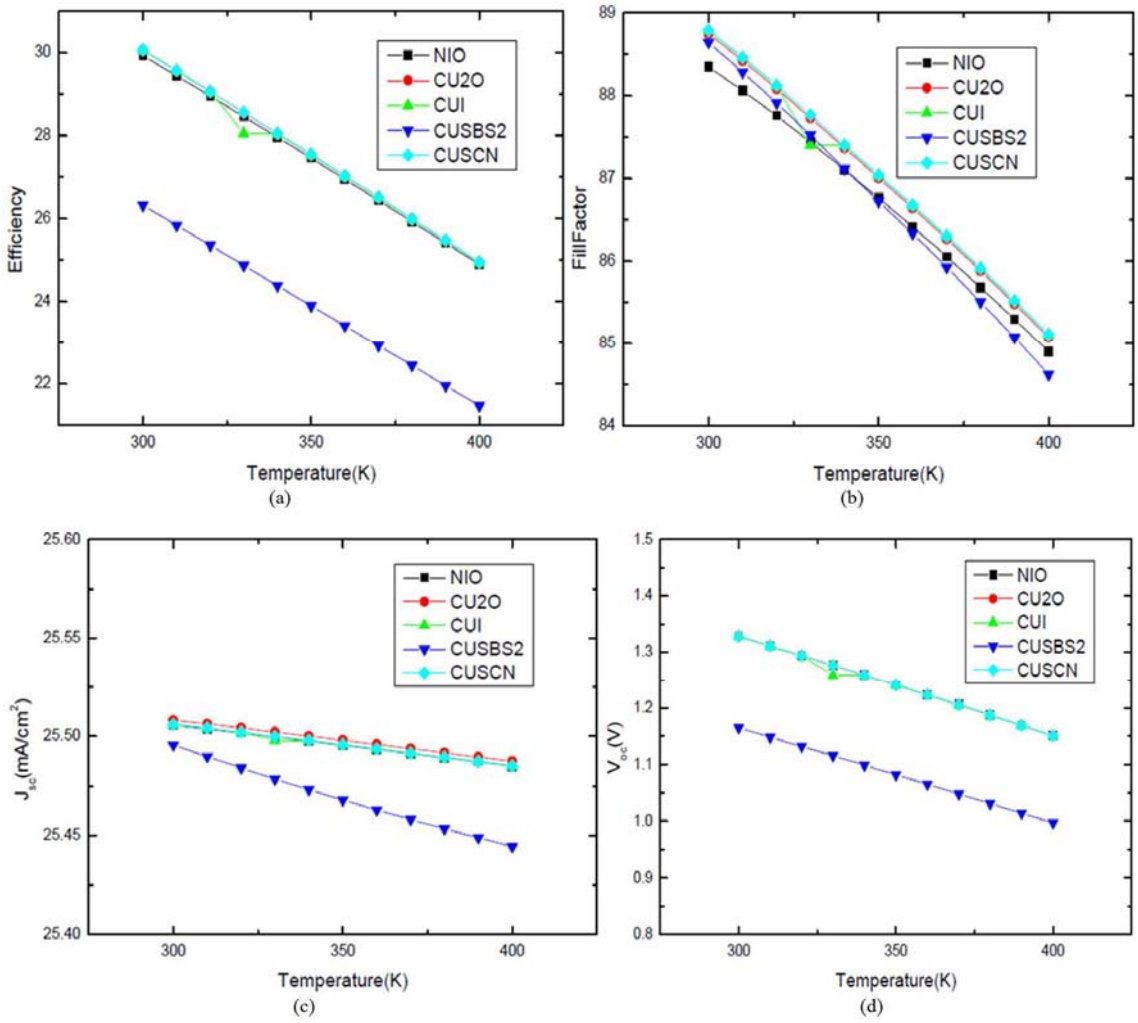

Figure 7. *Effect of variation of temperature on (a) PCE (b) FillFactor (c) J_{sc} and (d) Voc.*

V_{oc} decreased from 1.32 V to 1.14 V. This may be due to the rise in reverse saturation current, which decreases the voltage. So, 300 K temperature was used as working temperature for optimal performance. At this temperature the maximum achievable efficiency of the model is 30.01%, FillFactor is 88.87%, J_{sc}=25.58 mA/cm^2, and V_{oc}=1.32V.

3.5. Quantum Efficiency and J-V Characteristics

Figure 8 depicts the quantum efficiency (QE) curves of the various PSCs (a). It clearly shows that the studied PSCs have the same QE curve with minor variations. Almost the full visible range of the solar spectrum is covered by the QE curve. The QE is nearly constant in the region from 300 nm to 500 nm and then it decreases till 800 nm except for the device with NiO as the HTL. It should be pointed out here that the QE in SCAPS is the external QE. Figure 9 shows simulated J-V curves for the proposed PCE with optimised C_{60} as well as the absorber layer using various inorganic materials as HTL. Most of the combinations C_{60} /CuI, CuSCN, NiO, Cu_2O cell has a high open circuit voltage of 1.32V and short circuit current density (J_{sc}) of 25.99 mA/cm^2 respectively except $CuSbS_2$ which has a slightly lower open circuit voltage of 1.16V.

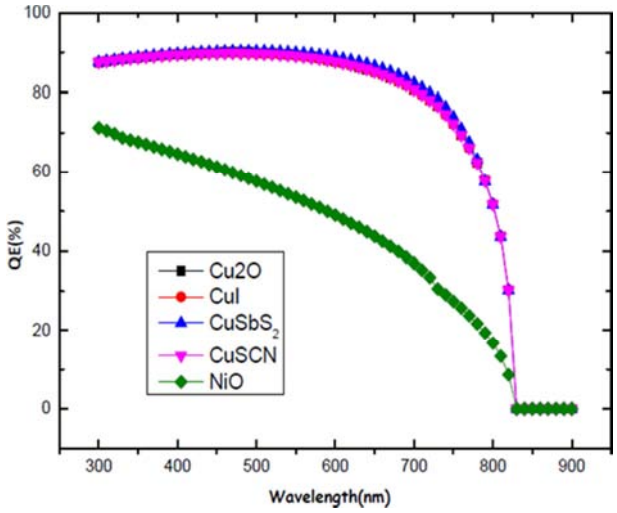

Figure 8. *QE curve of the simulated device with various HTLs.*

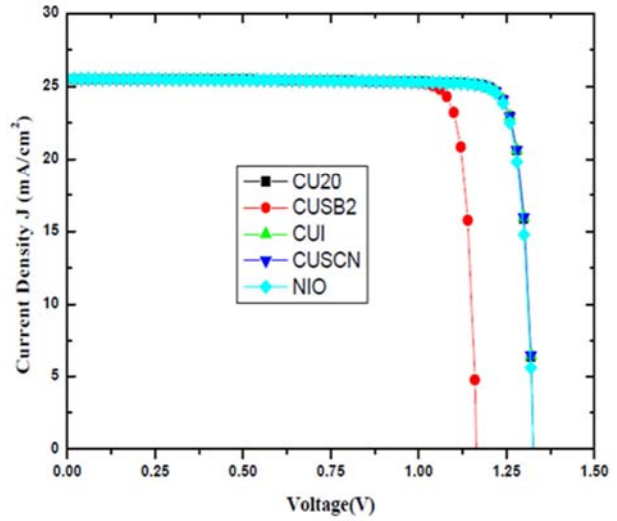

Figure 9. *Variation of J-V characteristics of proposed device with different HTMs.*

4. Conclusion

The solid-state perovskite solar cell models were controllably structured in SCAPS simulator and were successfully verified by comparing with performance parameters found in different literatures. The results show C_{60} as an alternate ETL having the potential to be used with $CsGeSnI_3$ absorber layer and can effectively replace organic ETLs which are expensive and easily degradable. We studied the various PV parameters with different HTM layers CuSCN, Cu_2O, NiO, $CuSbS_2$ and CuI with the proposed ETL (C_{60}) and absorber ($CsGeSnI_3$). After simulation we found that (i) C_{60} as ETL gives a considerable efficiency of 15.54% with $CsGeSnI_3$ (ii) the optimum thickness of C_{60} (ETL) and Absorber layer was found to 100nm and 500 nm respectively. (iii) 600 nm-700 nm of absorber was found to be appropriate to get better PV parameters; and (iv) the defect density in absorber should be maintained up to order of $10^{15}cm^{-3}$ (v) studied the effect of band gap variation and finally (vi) conclude that $CsGeSnI_3$ based PSC's are very sensitive to temperature. The increase in PSC temperature affects material conductivity which leads to the degradation of PV parameters. The device simulation being employed here not only substantiates our understanding obtained from these simulation results but also gives us a wider view in selecting the ETL materials. Our simulation will be useful for more deep understanding of the mechanism, material characterization, stability enhancing, and efficiency elevation of perovskite solar cells.

Acknowledgements

The author would like to acknowledge Nirmala College for the support. Also thank Professor Marc Burgelman and his colleagues in the Department of Electronics and Information Systems, University of Gent for the development of the SCAPS software package and allowing its use.

References

[1] Yoshikawa, K. *et al.* Silicon heterojunction solar cell with interdigitated back contacts for a photoconversion efficiency over 26%. *Nat. Energy* 2, 17032 (2017).

[2] Lead Iodide Perovskite Sensitized All-Solid-State Submicron Thin Film Mesoscopic Solar Cell with Efficiency Exceeding 9% | Scientific Reports. https://www.nature.com/articles/srep00591.

[3] Sequential deposition as a route to high-performance perovskite-sensitized solar cells | Nature. https://www.nature.com/articles/nature12340.

[4] Efficient and stable large-area perovskite solar cells with inorganic charge extraction layers | Science. https://science.sciencemag.org/content/350/6263/944.

[5] Correa-Baena, J.-P. *et al.* Promises and challenges of perovskite solar cells. *Science* 358, 739–744 (2017).

[6] Park, N.-G. Perovskite solar cells: an emerging photovoltaic technology. *Mater. Today* 18, 65–72 (2015).

[7] Kim, H.-S., Im, S. H. & Park, N.-G. Organolead Halide Perovskite: New Horizons in Solar Cell Research. *J. Phys. Chem. C*118, 5615–5625 (2014).

[8] Ahn, N. *et al.* Highly Reproducible Perovskite Solar Cells with Average Efficiency of 18.3% and Best Efficiency of 19.7% Fabricated via Lewis Base Adduct of Lead(II) Iodide. *J. Am. Chem. Soc.* 137, 8696–8699 (2015).

[9] Perovskite solar cells: an emerging photovoltaic technology – Science Direct. https://www.sciencedirect.com/science/article/pii/S1369702114002570.

[10] Stranks, S. D. *et al.* Electron-hole diffusion lengths exceeding 1 micrometer in an organometal trihalide perovskite absorber. *Science* 342, 341–344 (2013).

[11] Ahmed, S., Jannat, F., Khan, Md. A. K. & Alim, M. A. Numerical development of eco-friendly Cs2TiBr6 based perovskite solar cell with all-inorganic charge transport materials via SCAPS-1D. *Optik* 225, 165765 (2021).

[12] Mandadapu, U., Vedanayakam, S. V., Thyagarajan, K. & Babu, B. j. Optimisation of high efficiency tin halide perovskite solar cells using SCAPS-1D. *Int. J. Simul. Process Model.* 13, 221–227 (2018).

[13] Manceau, M., Rivaton, A., Gardette, J.-L., Guillerez, S. & Lemaître, N. Light-induced degradation of the P3HT- based solar cells active layer. *Sol. Energy Mater. Sol. Cells* 95, 1315–1325 (2011).

[14] Jiang, K., Wu, F., Zhang, G., Zhu, L. & Yan, H. Efficient Perovskite Solar Cells Based on Dopant-Free Spiro-OMeTAD Processed With Halogen-Free Green Solvent. *Sol. RRL*3, 1900061 (2019).

[15] A dopant-free organic hole transport material for efficient planar heterojunction perovskite solar cells - Journal of Materials Chemistry A (RSC Publishing). https://pubs.rsc.org/en/content/articlelanding/2015/ta/c5ta02502h/unauth#!divAbstract.

[16] Chen, Y. *et al.* SnO_2-based electron transporting layer materials for perovskite solar cells: A review of recent progress. *J. Energy Chem.* 35, 144–167 (2019).

[17] Jung, M. *et al.* Thermal Stability of CuSCN Hole Conductor-Based Perovskite Solar Cells. *Chem Sus Chem* 9, 2592–2596 (2016).

[18] Perovskite solar cells with CuSCN hole extraction layers yield stabilized efficiencies greater than 20% | Science. https://science.sciencemag.org/content/358/6364/768.

[19] Formation of pristine CuSCN layer by spray deposition method for efficient perovskite solar cell with extended stability - ScienceDirect. https://www.sciencedirect.com/science/article/abs/pii/S221128551630622X.

[20] Cesium-containing triple cation perovskite solar cells: improved stability, reproducibility and high efficiency - Energy & Environmental Science (RSC Publishing). https://pubs.rsc.org/en/content/articlelanding/2016/ee/c5ee03874j#!divAbstract.

[21] Islam, M. T. *et al.* Numerical simulation studies of a fully inorganic Cs2AgBiBr6 perovskite solar device. *Opt. Mater.* 105, 109957 (2020).

[22] Continuous Grain-Boundary Functionalization for High-Efficiency Perovskite Solar Cells with Exceptional Stability - ScienceDirect. https://www.sciencedirect.com/science/article/pii/S2451929418301189.

[23] Du, K., Meng, W., Wang, X., Yan, Y. & Mitzi, D. B. Bandgap Engineering of Lead-Free Double Perovskite Cs2AgBiBr6 through Trivalent Metal Alloying. *Angew. Chem. Int. Ed.* 56, 8158–8162 (2017).

[24] High-Quality Sequential-Vapor-Deposited Cs2AgBiBr6 Thin Films for Lead-Free Perovskite Solar Cells - Wang - 2018 - Solar RRL - Wiley Online Library. https://onlinelibrary.wiley.com/doi/abs/10.1002/solr.201800217.

[25] Cesium Titanium(IV) Bromide Thin Films Based Stable Lead-free Perovskite Solar Cells - ScienceDirect. https://www.sciencedirect.com/science/article/pii/S2542435118300370.

[26] Ju, M.-G. *et al.* Earth-Abundant Nontoxic Titanium(IV)-based Vacancy-Ordered Double Perovskite Halides with Tunable 1.0 to 1.8 eV Bandgaps for Photovoltaic Applications. *ACS Energy Lett.* 3, 297–304 (2018).

[27] Heterojunction-Depleted Lead-Free Perovskite Solar Cells with Coarse-Grained B-γ-CsSnI3 Thin Films – Wang.

[28] Advanced Energy Materials - Wiley Online Library. https://onlinelibrary.wiley.com/doi/abs/10.1002/aenm.201601130.

[29] MAPbI3 and FAPbI3 perovskites as solar cells: Case study on structural, electrical and optical properties - ScienceDirect. https://www.sciencedirect.com/science/article/pii/S2211379718311811.

[30] Enhanced stability and efficiency in hole-transport-layer-free CsSnI 3 perovskite photovoltaics | Nature Energy. https://www.nature.com/articles/nenergy2016178.

[31] Highly stable and efficient all-inorganic lead-free perovskite solar cells with native-oxide passivation | Nature Communications. https://www.nature.com/articles/s41467-018-07951-y.

[32] Shao, S. *et al.* Highly Reproducible Sn-Based Hybrid Perovskite Solar Cells with 9% Efficiency. *Adv. Energy Mater.* 8, 1702019 (2018).

[33] CsSnI3: Semiconductor or Metal? High Electrical Conductivity and Strong Near-Infrared Photoluminescence from a Single Material. High Hole Mobility and Phase-Transitions - Google Search. https://www.google.com/search?client=firefox-b-d&q=CsSnI3%3A+Semiconductor+or+Metal%3F+High+Electrical+Conductivity+and+Strong+Near-Infrared+Photoluminescence+from+a+Single+Material.+High+Hole+Mobility+and+Phase-Transitions.

[34] Roy, P. & Khare, A. Analysis of an efficient and eco-friendly CsGeSnI3 based perovskite solar cell: A theoretical study. *Mater. Today Proc.* 44, 2997–3000 (2021).

[35] Raghvendra, Kumar, R. R. & Pandey, S. K. Performance evaluation and material parameter perspective of eco-friendly highly efficient CsSnGeI3 perovskite solar cell. *Superlattices Microstruct.* 135, 106273 (2019).

[36] Raj, A., Kumar, M., Bherwani, H., Gupta, A. & Anshul, A. Evidence of improved power conversion efficiency in lead-free CsGeI3 based perovskite solar cell heterostructure via scaps simulation. *J. Vac. Sci. Technol. B*39, 012401 (2020).

[37] Kancharla, S. & Kaushik, D. K. Optimization of electrical and optical properties of tin sulfide for thin film photovoltaics using SCAPS. *J. Phys. Conf. Ser.* 1531, 012016 (2020).

[38] Mouchou, R. T., Jen, T. C., Laseinde, O. T. & Ukoba, K. O. Numerical simulation and optimization of p-NiO/n- TiO2 solar cell system using SCAPS. *Mater. Today Proc.* 38, 835–841 (2021).

[39] Burgelman, M., Nollet, P. & Degrave, S. Modelling polycrystalline semiconductor solar cells. *Thin Solid Films* 361–362, 527–532 (2000).

[40] Decock, K., Khelifi, S. & Burgelman, M. Modelling multivalent defects in thin film solar cells. *Thin Solid Films* 519, 7481–7484 (2011).

[41] Verschraegen, J. & Burgelman, M. Numerical modeling of intra-band tunneling for heterojunction solar cells in scaps. *Thin Solid Films* 515, 6276–6279 (2007).

[42] (PDF) Simulation and Analysis of Methylammonium Lead Iodide (CH3NH3PbI3) Perovskite Solar Cell with Au Contact Using SCAPS 1D Simulator. https://www.researchgate.net/publication/336409486_Simulation_and_Analysis_of_Methylammonium_Lead_Iodide_CH3NH3PbI3_Perovskite_Solar_Cell_with_Au_Contact_Using_SCAPS_1D_Simulator.

[43] Investigating the Effect of ZnSe (ETM) and Cu2O (HTM) on Absorber Layer on the Performance of Pervoskite Solar Cell Using SCAPS-1D:: Science Publishing Group. http://www.sciencepublishinggroup.com/journal/paperinfo?journalid=622&doi=10.11648/j.ajpa.20200801.12.

[44] Chakraborty, K., Choudhury, M. G. & Paul, S. Numerical study of Cs2TiX6 (X = Br−, I−, F− and Cl−) based perovskite solar cell using SCAPS-1D device simulation. *Sol. Energy* 194, 886–892 (2019).

[45] Azadinia, M., Ameri, M., Ghahrizjani, R. T. & Fathollahi, M. Maximizing the performance of single and multijunction MA and lead-free perovskite solar cell. *Mater. Today Energy* 20, 100647 (2021).

[46] Olopade, M., Adewoyin, A., Chendo, M. & Bolaji, A. The Study of Some Materials as Buffer Layer in Copper Antimony Sulphide (CUSbS2) Solar Cell Using SCAPS 1-D. in *2017 IEEE 44th Photovoltaic Specialist Conference (PVSC)* 2381–2384 (2017). doi: 10.1109/PVSC.2017.8366580.

[47] Nithya, K. S. & Sudheer, K. S. Device modelling of non-fullerene organic solar cell with inorganic CuI hole transport layer using SCAPS 1-D. *Optik* 217, 164790 (2020).

[48] Sawicka-Chudy, P., Sibiński, M., Wisz, G., Rybak-Wilusz, E. zbieta & Cholewa, M. Numerical analysis and optimization of Cu_2O/TiO_2, CuO/TiO_2, heterojunction solar cells using SCAPS. *J. Phys. Conf. Ser.* 1033, 012002 (2018).

[49] A Tin-Based Perovskite Solar Cell With an Inverted Hole-Free Transport Layer to Achieve High Energy Conversion Efficiency by & nbsp; SCAPS Device Simulation | Research Square. https://www.researchsquare.com/article/rs-338951/v1.

[50] Effect of different device parameters on tin-based perovskite solar cell coupled with In2S3 electron transport layer and CuSCN and Spiro-OMeTAD alternative hole transport layers for high-efficiency performance: Energy Sources, Part A: Recovery, Utilization, and Environmental Effects: Vol 0, No 0. https://www.tandfonline.com/doi/abs/10.1080/15567036.2020.1820628.

[51] Toshniwal, A., Jariwala, A., Opanasyuk, A., Panchal, C. & Kheraj, V. *Numerical simulation of tin based perovskite solar cell: Effects of absorber parameters and hole transport materials*. (2017).

[52] Azizi, T., Toujeni, H., Ben Karoui, M. & Gharbi, R. A comprehensive device modeling of solid state dye sensitized solar cell with SCAPS-1D. in *2019 19th International Conference on Sciences and Techniques of Automatic Control and Computer Engineering (STA)* 336–340 (2019). doi: 10.1109/STA.2019.8717282.

[53] Abdelfatah, M., Ismail, W., El-Shafai, N. M. & El-Shaer, A. Effect of thickness, bandgap, and carrier concentration on the basic parameters of Cu_2O nanostructures photovoltaics: numerical simulation study. *Mater. Technol.* 0, 1–9 (2020).

[54] Kumar, M. *et al.* Organic-inorganic perovskite-based solar cell designs for high conversion efficiency: A comparative study by SCAPS simulation. *Mater. Today Proc.* (2020) doi: 10.1016/j.matpr.2020.11.035.